water

MDPI

Review

Advances in High-Performance Nanofiltration Membranes Facilitated by Two-Dimensional Materials

Sichu Xing [1,2], Songhang Du [1], Yingyue Huang [1], Xingqi Qi [1] and Minghao Sui [1,*]

[1] State Key Laboratory of Pollution Control and Resource Reuse, School of Environmental Science and Engineering, Tongji University, 1239 Siping Road, Shanghai 200092, China; xingsichu@smedi.com (S.X.); deeesoooh@163.com (S.D.); 2130487@tongji.edu.cn (Y.H.); 2132841@tongji.edu.cn (X.Q.)
[2] Shanghai Municipal Engineering Design Institute (Group) Co., Ltd., Shanghai 200092, China
* Correspondence: minghaosui@tongji.edu.cn; Tel.: +86-21-65982691

Abstract: Nanofiltration membranes (NF) have been widely used in the field of water treatment because of their advantages of high separation precision, easy operation, and no phase change. Conventional NF membranes, ensnared by the "trade-off" effect, grapple with the challenge of achieving breakthroughs in both separation efficacy and stability. Recent advancements in research have unveiled the potential of nanoscale porous two-dimensional (2D) materials, characterized by their atomic thinness and superlative mechanical strength. These materials, crafted into nanofiltration membranes as thin as a single atom, boast minimal transport resistance and maximal permeation flux, thereby facilitating the highly discerning transport of water, and are heralded as the quintessential materials for fabricating ultra-thin membranes. This comprehensive review delves into the latest advancements in the research on 2D material NF membranes. A range of performance aspects related to 2D-material-modified NF membranes, including water flux, permeability, pollutant retention rates, and anti-pollution performance, were evaluated, and this review covers the impact of and major approaches to optimizing membrane performance in recent years, providing valuable insights into potential future developments in NF membranes.

Keywords: nanofiltration membrane; two-dimensional materials; membrane modification; high flux; improved antifouling performance

Citation: Xing, S.; Du, S.; Huang, Y.; Qi, X.; Sui, M. Advances in High-Performance Nanofiltration Membranes Facilitated by Two-Dimensional Materials. *Water* **2024**, *16*, 988. https://doi.org/10.3390/w16070988

Academic Editor: Anastasios Zouboulis

Received: 21 February 2024
Revised: 24 March 2024
Accepted: 25 March 2024
Published: 28 March 2024

1. Introduction

In the current milieu, the relentless surge in population and the rapid pace of economic development are pitted against the backdrop of finite natural resources, thrusting water pollution and freshwater scarcity to the forefront as pressing challenges [1]. Projections indicate that, by 2050, a staggering 4 to 5 billion people globally will grapple with water shortages and waterborne diseases [2]. The emergence of the COVID-19 pandemic in 2019 has further underscored potential health risks associated with freshwater and sewage pollution. One of the Sustainable Development Goals (2015–2030), number six, is to provide "clean, accessible water for all", demanding innovative materials and technologies for producing clean water from alternative sources such as wastewater, seawater, and brackish water [3]. As a cost-effective and energy-efficient method of water purification, membrane separation technology has garnered significant attention due to its simple operational processes, high separation efficiency, and widespread applicability in areas such as drinking water production, urban and industrial wastewater treatment, resource recovery, and material separation and concentration [4–6]. Depending on pore size, pressure-driven membrane separation processes include microfiltration (MF), ultrafiltration (UF), nanofiltration (NF), and reverse osmosis (RO) [7–10]. The molecular weight cutoff of NF membranes falls between 200 and 2000 Da, positioning them between RO and UF membranes. The unique ion selectivity and substantial membrane flux of NF membranes confer advantages such as a low operating pressure and high water purification efficiency. They can not only

remove low molecular weight organic compounds and inorganic salts but also effectively adsorb heavy metal ions, making them widely applicable in water treatment. Nanofiltration membranes also bear abundant surface charges, potentially playing a pivotal role in repelling charged solutes [11–13].

Nevertheless, a persistent "trade-off" effect exists between the permeability and separation performances of NF membranes, where membrane permeation flux and the retention rate prove challenging to balance, constraining each other. Achieving the ultra-thinning of the separation layer while ensuring membrane integrity emerges as a pivotal approach to breaking the "trade-off" effect. However, the ultra-thin nature of the separation layer poses challenges to the structure of the membrane and its stability. Furthermore, membrane fouling is an inevitable occurrence in practical applications, leading to diminished separation efficiency, compromised membrane stability, and increased operational maintenance costs [14–19]. Addressing the trade-off dilemma by designing novel membrane materials that concurrently enhance selectivity, permeability, and stability has become a pressing issue in the field of dense membranes. In recent years, the widespread research interest in two-dimensional (2D) material NF membranes has surged due to their tunable pore sizes, geometric structures, chemical properties, excellent chemical resistance, sufficient mechanical strength, and outstanding fouling resistance [20–22].

Compared to traditional polymeric materials, 2D materials offer a multitude of distinct advantages. (1) The unique single- to few-atom thickness morphologies of 2D nanosheets allow them to serve as ideal building blocks, enabling precise thickness control and the design of membrane transport properties [23–26]. (2) The narrow interlayer spacing between 2D material nanosheets makes achieving specific molecular selectivity possible [27–29]. (3) The ability of 2D materials to form slit-like nanochannels facilitates molecular transport in confined nanoscale spaces (spaces < 2 nm), sometimes leading to unexpected abnormal infiltration phenomena. The ultrafast water and ion permeation rates are orders of magnitude higher than those in graphene oxides (GO) membranes [30]. (4) The tunable physicochemical properties and interlayer spacing/nanopores of 2D materials provide a broader window for membrane design [31–33]. (5) Some 2D materials exhibit outstanding chemical resistance in harsh chemical environments, making the manufacturing and application of membranes feasible in various separation processes [27,28,34]. These characteristics position 2D materials as promising candidates for the fabrication of high-performance membrane-separation applications [35–39]. Notable hot topics in the research on 2D materials include graphene [40], GO [41], reduced graphene oxides (rGO) [42], the family of two-dimensional transition metal carbides, nitrides, and carbonitrides (MXenes) [43], 2D metal-organic frameworks (MOF) [44], and 2D covalent organic frameworks (COF), among others. The rapidly evolving landscape of 2D materials provides a diverse new material platform capable of propelling breakthroughs in NF membrane research [45,46].

This review investigated the recent progress in the research on 2D material NF membranes. A systematic assessment was conducted on various performance aspects of 2D-material-modified NF membranes, such as water flux, permeability, pollutant retention rates, and anti-pollution performance. Our analysis covers the impact of and key methods for enhancing NF membrane performance in recent years, offering valuable insights into potential future advancements in NF membranes.

2. Separation Mechanism and Preparation Methods of 2D Material Nanofiltration Membranes

Two-dimensional materials function as nanofillers (solid phase), dispersed within a continuous matrix (polymer phase) of the polymer substrate. The introduction of 2D materials induces the creation of interface gaps between polymer chains and nanofillers (Figure 1) [47–49]. These gaps provide additional channels for molecular transport, endowing the membrane with a higher permeability compared to pure polymer membranes. A small number of 2D nanosheets with specific interlayer spacing can act as nanochannels

for molecular transport [36,50–53]. Two-dimensional material NF membranes can be categorized into two groups, i.e., layered membranes, which mainly depend on interlayer channel pathways for permeation, and membranes made of porous nanosheets. And the separation mechanism of 2D material NF membrane depends largely on the assembly of 2D materials in the membrane [36,46,54].

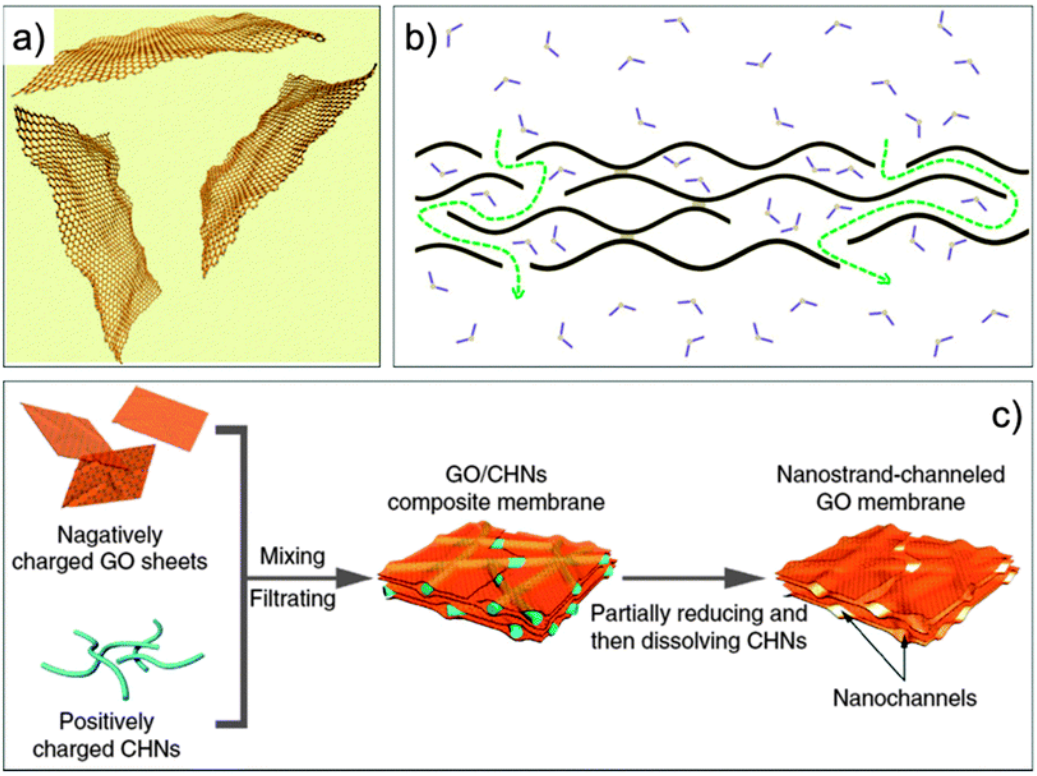

Figure 1. (**a**) Schematic representation of graphene sheets suspended in a liquid, displaying the potential for corrugation; (**b**) illustration depicting water molecules traversing a corrugated chemically converted graphene membrane, with dashed lines indicating potential water flow paths. Reprinted with permission from Ref. [55]. 2011, Copyright RSC. (**c**) A depiction of the manufacturing process for a nanostrand-channelled GO membrane (CHN: copper hydroxide nanostrands). Reprinted with permission from Ref. [56]. 2013, Copyright Springer Nature limited.

2.1. Laminar Membrane

To fully exploit their morphological advantages, 2D nanosheets are typically assembled into 2D laminar membranes. In laminar membranes, precise control over the size of the permeating molecules, permeation rate, and selectivity is achieved through the manipulation of convoluted paths between uniformly sized nano-layered plates, forming tunable nanochannels. Laminar membranes typically have two transport pathways: horizontal and vertical nanochannels. Horizontal nanochannels consist of interlayer pathways formed by two adjacent 2D nanosheets (Figure 2). The explicit interlayer spacing of horizontal nanochannels allows for the exertion of size-exclusion effects. To achieve the desired membrane performance, precisely adjusting the interlayer spacing to obtain tunable nanochannel pores has become a primary means of the fabrication of 2D material membranes, particularly for those assembled from non-porous 2D materials. Ions and molecules traverse the interlayer spacing formed by adjacent 2D nanosheets, where functional groups also play a crucial role in molecular transport. For instance, in laminar GO membranes, oxygen-containing functional groups on the basal plane form hydrogen bonds with water molecules, increasing water permeation [57,58]. These oxygen-containing groups also maintain the interlayer spacing between non-oxidized regions, which, at the nanoscale, provide a capillary network. Membranes crafted from other 2D materials such as

rGO, MXenes, and 2D transition metal dichalcogenides also show similar water transport pathways. The high performance of laminar 2D material NF membranes hinges primarily on the regulation of interlayer spacing and material functionality. Numerous studies report the adjustment of MXene nanosheet interlayer spacing through cation intercalation [59,60]. For instance, in a study by Ding et al. [61], Al^{3+} cations were intercalated into the interlayers of Ti_3C_2 MXene nanosheets. This intercalation significantly improved their ion rejection properties. The intercalated MXene membranes exhibit a remarkable capacity to reject NaCl (~89.5–99.6%) while maintaining fast water fluxes (~1.1–8.5 $L \cdot m^{-2} \cdot h^{-1}$) [62].

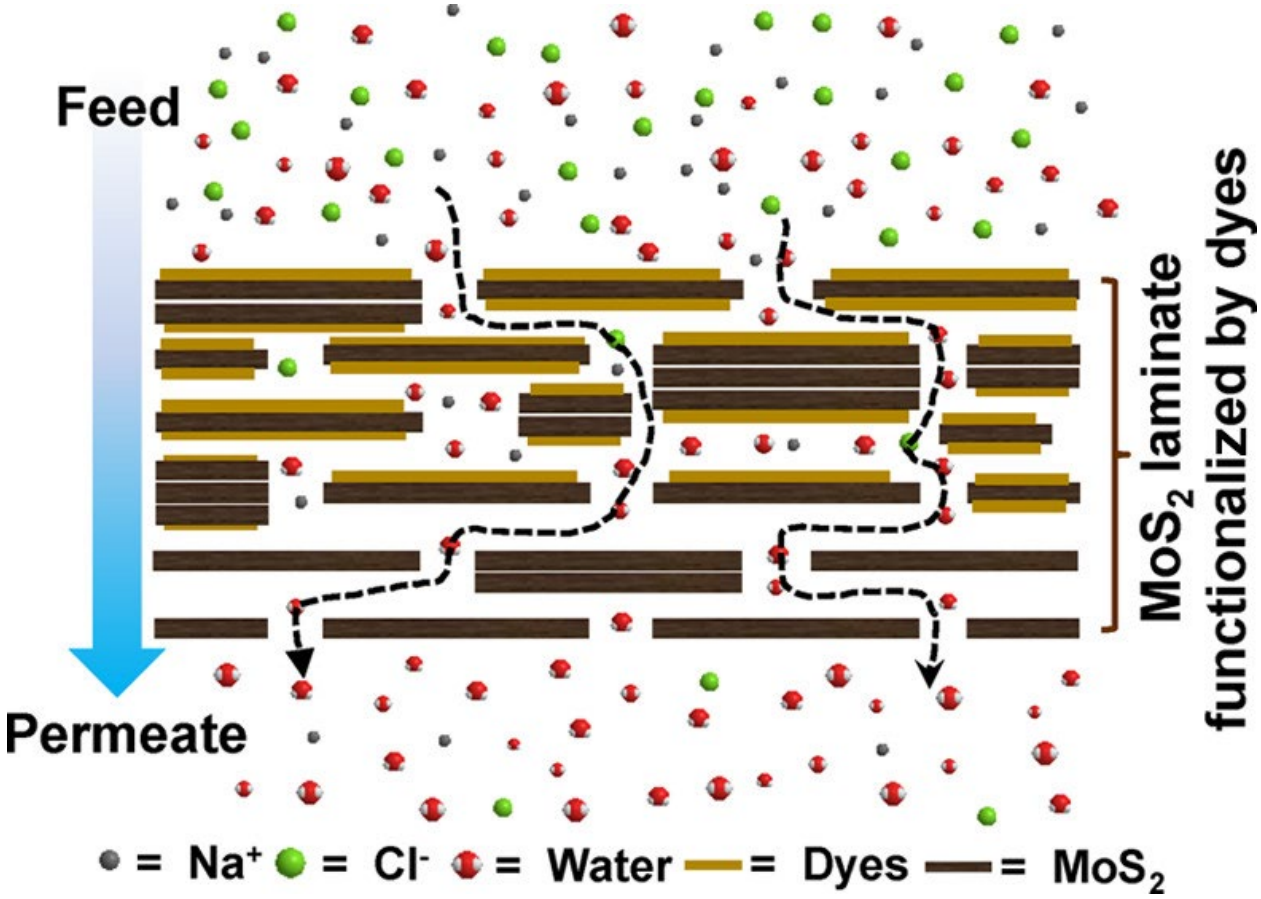

Figure 2. Schematic showing the diffusion, driven by the large concentration gradient, of the solute (Na^+ and Cl^- ions in this case) through the MoS_2 laminar membrane which has been prefunctionalized by organic dye. Reprinted with permission from Ref. [63]. 2017, Copyright ACS.

While the controllable interlayer spacing enables the regulation of membrane pores to facilitate molecular transport, intrinsic defects in 2D nanosheets, such as high aspect ratios and curved nanochannels, increase the length of the transmission path [22,64]. Vertical nanochannels alleviate these issues to some extent, including in-plane pores (defects) on the basal plane of 2D material nanosheets, nano-stones formed in the edge gaps of 2D material nanosheets, and intrinsic pores in 2D materials. For example, in-plane pores on the basal plane of graphene nanosheets provide additional vertical nanochannels, creating transmission shortcuts (Figure 3) [65]. Additionally, inherently porous 2D materials, such as 2D COFs, can offer abundant vertical nanochannels [66].

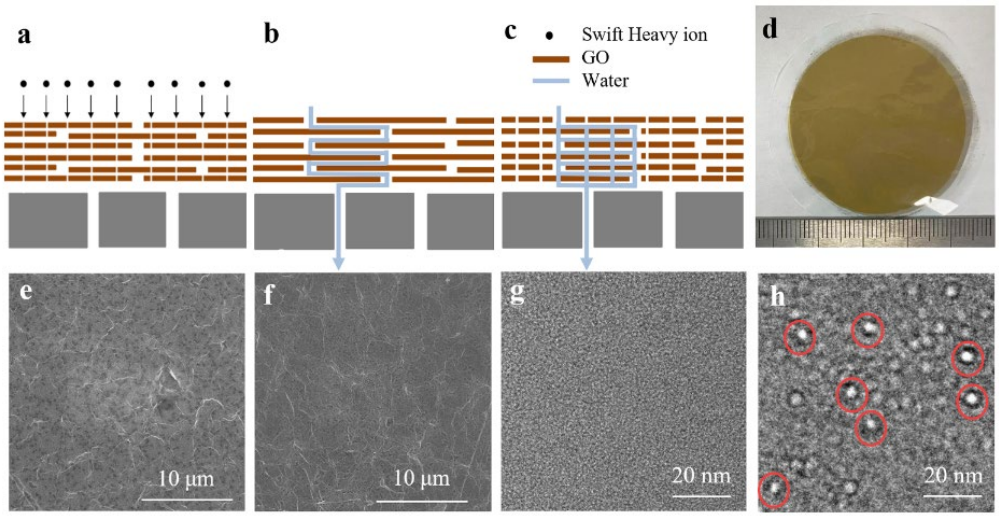

Figure 3. (**a**) Schematic diagram of GO membrane (GOM) irradiated by swift heavy ions for the construction vertical nanochannels. Schematic diagrams of water flow path of (**b**) pristine GOM and (**c**) GOM after ion irradiation. (**d**) Photographs of GOM-5E11-Kr. SEM images of (**e**) GOM and (**f**) GOM-5E11-Kr. TEM image of (**g**) GOM and (**h**) GOM-2E11-Xe. The nanopores are marked with red circles (GOM-5E11-Kr means that the GOM was irradiated by Kr ions with the fluence of 5×10^{11} ions cm^2, and GOM-2E11-Xe means that the GOM was irradiated by Xe ions with the fluence of 2×10^{11} ions cm^2. Reprinted with permission from Ref. [65]. 2023, Copyright Elsevier).

2.2. Nanoporous Membrane

Another category of 2D nanofiltration membranes features a nanoporous pathway structure that acts as a precise molecular sieve through the provision of pores, allowing water molecules to pass while excluding other ions (Figure 4) [67]. Due to their atomic thinness, ions (for example, Na^+, K^+, and Cl^-) can permeate with minimal transport resistance, thereby enhancing water permeation. Commonly, these membranes are more suitable for the retention of most divalent ions and larger molecules than traditional nanofiltration membranes. Still, with aperture adjustments, some monovalent molecules can also be removed [68]. The separation mechanism of 2D material NF membranes primarily relies on size exclusion and electrostatic interactions [69]. Depending on membrane modifications and separation applications, ions can also be retained through ion adsorption [70–72]. After the first introduction of nanoporous graphene into NF membrane [73], h-BN (hexagonal boron nitride, also known as white graphene) and compounds with inherent porosity, including 2D zeolites, 2D MOFs, covalent triazine frameworks (CTFs), graphitic carbon nitride (g-C_3N_4), and COFs, are brought into NF membranes to improve their filtration performance, adhering to the separation mechanisms described above. Materials with inherent porosity avoid the need for a pore generation process, exhibiting higher filtration performance [74]. In recent years, modifications to existing membranes using nanoporous materials have opened up new possibilities for improving nanofiltration processes. Chi et al. presented a polyamide (PA) composite nanofiltration membrane modified by a nanoporous TiO_2 interlayer to improve water permeability, showcasing the potential of enhancing separation efficiency through membrane modifications [75]. The modified membrane had a permeability of 12.8 $L \cdot m^{-2} \cdot h^{-1} \cdot bar^{-1}$, which was an increase of 20.8% compared to that of polyamide composite (TFC membrane), and a rejection rate of 98.2% when filtering a Na_2SO_4 aqueous solution. In addition to material innovations, the functionalization of nanoporous membranes was reported to improve the filtration properties. A functionalized nanoporous graphene (FNG) membrane, which was prepared by functionalizing GO with oxygen-containing groups via $KMnO_4$ treatment, was reported to exhibit a water permeance of 586 $L \cdot m^{-2} \cdot h^{-1} \cdot bar^{-1}$ and a precise molecular separation (molecular weight cutoff: 269 Da) due to the synergistic effect of nanopores and oxygen-containing groups [76]. Researchers have been focusing on tuning nanopores to enhance their filtration perfor-

mance [54]. Li et al. [77] reported the synthesis of large-area defect-free COF membranes with uniformly distributed subnanopores via a simple wet-chemical reaction. This work demonstrated a scalable fabrication method to grow COF membranes with tunable pore sizes in the sub-nm region. Two-dimensional ZTC was bottom-up synthesized through carbon deposition on presynthesized IWV zeolite (Si/Al = 28) using acetylene as a carbon source and subsequent zeolite etching with a NaOH solution [78]. The resulting carbon is made of an extremely thin polyaromatic backbone and contains well-defined vertically aligned micropores (0.69 nm in diameter). In a similar work, Zhao et al. [79] developed colloidal 2D COF membranes with tailored thicknesses and surface charges for precise molecular sieving by oil-in-water emulsion interfacial polymerization technology.

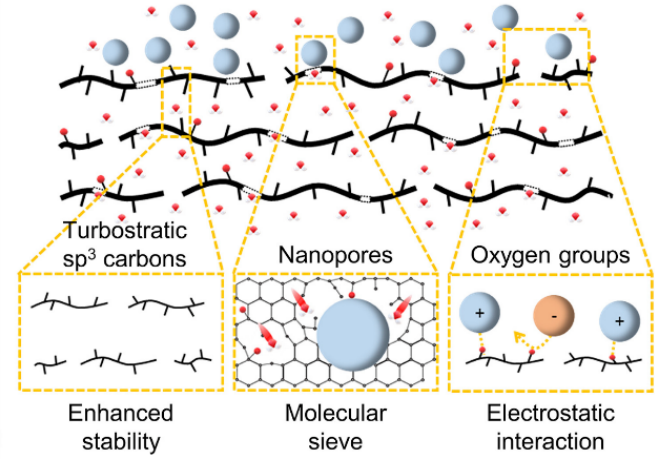

Figure 4. Schematic of porous nanosheet membrane: nanofiltration mechanism of functionalized nanoporous graphene membrane. Reprinted with permission from Ref. [76]. 2021, Copyright Elsevier.

2.3. Fabrication Methods

The performance of membranes relies on their structural and physicochemical properties, encompassing thickness, pore size, and porosity, as well as surface charge density, hydrophilicity, and roughness. Understanding the relationship between membrane performance and these properties, as well as how membrane performance is influenced by manufacturing methods and conditions, will contribute to tailoring nanofiltration membranes for various application domains [80].

The blending method involves uniformly incorporating two-dimensional nanomaterials into the precursor solution of the membrane material. By employing methods such as phase transformation [81], vapor-phase polymerization sol-gel, and others, a continuous membrane is formed to prepare a composite membrane with uniformly dispersed two-dimensional nanomaterials. This method offers the advantages of technological maturity, operational simplicity, and good stability of the membrane materials. Vatanpour et al. [82] used a blending method to enhance the permeability, fouling resistance, antibacterial properties, separation capability, and mechanical strength of polyethersulfone (PES) membranes by incorporating a two-dimensional nanocomposite material composed of functionalized h-BN nanosheets/graphene oxide/silver (FBN-GO-Ag). First, BN-GO-Ag NPs were added to dimethylacetamide and sonicated until a complete dispersion of BN-GO-Ag was reached. Then, polyvinylpyrrolidone polymer was added and stirred. Finally, PES was poured into the solution and stirred until it dissolved completely. After degassing, the polymeric solutions were poured over the cleaned glasses, and were then rapidly soaked in a water bath. The hydrophilicity and porosity of the modified membrane increased, and the permeability increased by 40%, accompanied by improvements in its dye removal and antifouling properties. In comparison to zero-dimensional, one-dimensional, and three-dimensional materials, the stacking and mutual contact of two-dimensional nanomaterials in blended

membranes can more effectively guide the flow of water molecules, enhance separation, and simultaneously create pathways for the rapid migration of charge carriers [83].

The self-assembly technique based on filtration is currently the most commonly used method for fabricating 2D material membranes, offering simplicity and high controllability. The self-assembly technique is a process in which a disordered system of preexisting components forms an organized structure or pattern due to specific, local interactions among the components themselves, without external direction. Filtration pressure operates in two modes: pressure-assisted filtration and vacuum-assisted filtration. The filtration mode significantly influences the microstructure of the resulting laminar membrane. Laminar structures generated through pressure-assisted filtration exhibit highly ordered and densely compacted uniform stacking, which is the result of sustained pressure ensuring stable compression. In contrast, nanosheets produced through vacuum-assisted filtration have a looser assembly due to the decreasing vacuum suction when nanosheets reassemble during the filtration process [84]. Moreover, the dispersion of laminar structures in water or organic solvents can significantly impact the integrity of laminar membranes. For these reasons, filtration is widely employed in the fabrication of membranes based on GO. The hydrophilic nature of GO nanosheets allows for their effective dispersion in water or most polar organic solvents, facilitating the formation of highly ordered laminar structures [25–27]. Furthermore, by adjusting the volume and concentration of the 2D material dispersion, membrane thickness is easily controlled, making filtration an easily implementable and cost-effective method. These characteristics render filtration a versatile approach, and it is extensively utilized in the manufacturing of 2D material membranes [23,31,34,85].

Layer-by-Layer (LbL) assembly involves the alternating deposition of 2D materials with opposite charges, making it highly suitable for the fabrication of dense multilayer membranes with adjustable thickness and functionality (Figure 5). Multilayer membranes assembled on a substrate can be further stabilized through covalent bonding, hydrogen bonding interactions, and other molecular interactions. The number of deposition cycles can precisely control the thickness of laminar membranes, and the electrostatic interactions between layers may help alleviate swelling in organic solvents [86,87]. Therefore, LbL is an attractive preparation method that has expanded its applications from highly charged functional groups in GO to other 2D materials, such as MoS_2 [88].

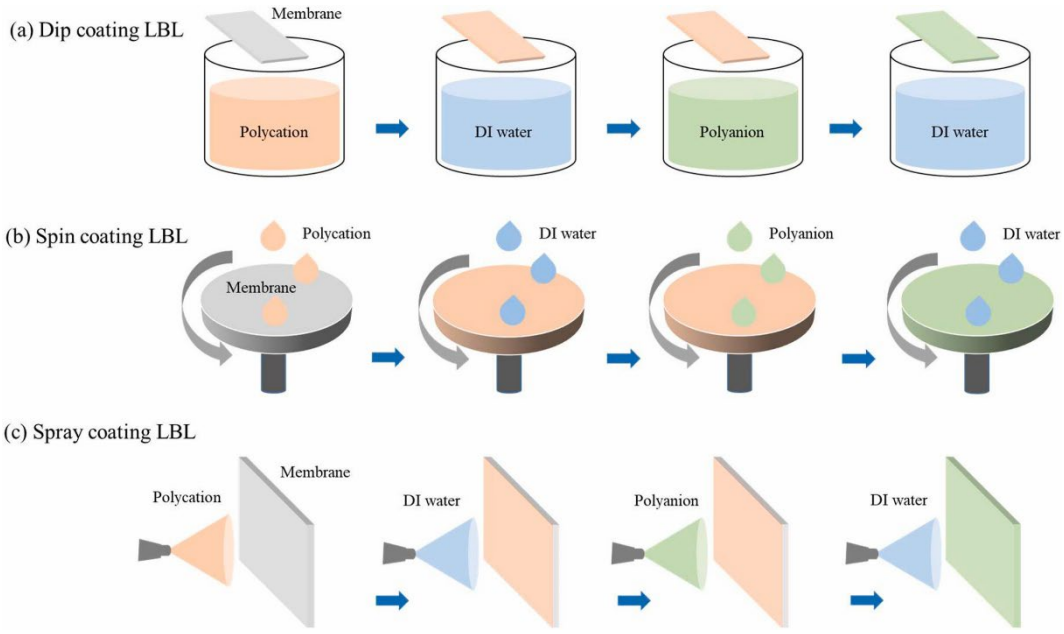

Figure 5. Schematic diagrams of the conventional LBL assembly methods. Reprinted with permission from Ref. [89]. 2022, Copyright Elsevier.

Furthermore, coating, mixing, and casting are also employed to obtain 2D material membranes [90–93]. Typically, 2D materials need to exhibit a good dispersibility in solvents to retain their 2D morphology during film-forming processes using these methods. However, some 2D materials, such as 2D COFs, are challenging to process into defect-free continuous membranes due to their relatively poor dispersibility in water and organic solvents. Therefore, some reports have explored alternative methods like in situ growth [28], interface polymerization [29], and the Langmuir–Blodgett method [30]. In summary, the current focus of most research is still on the ability to precisely control the structure of 2D material NF membranes. In contrast, there is much less research on the scalability of manufacturing methods, except for membranes based on graphene materials. The scalability of manufacturing methods will be a key factor in advancing the practical applicability of 2D material membranes.

3. Typical Nanofiltration Membranes with 2D Materials and Their Filtration Performance

The research on the new generation of nanomaterials dominated by carbon-based nanomaterials and porous nanomaterials has been progressing rapidly and is gradually being applied to nanofiltration membrane modification, which is able to regulate the pores in the sub-nanometer range to control the transport properties [94–100]. The two-dimensional structure has the advantages of large specific surface area, tunable layer spacing, and good hydrophilicity, which can effectively avoid structural complexity and compositional inhomogeneity [101], as well as the ability to generate high-density nanopores (approximately 10^{12} cm^{-2}) to confer polymer permeability. In addition, the membranes typically exhibit high mechanical strength and broad chemical compatibility, and are not disturbed by problems such as dissolution or swelling in harsh chemical environments and extreme operating conditions, with the potential to transform the technology into useful membrane separations.

3.1. Graphene-Based NF Membranes

Since the first discovery of graphene by A. K. Geim and K. S. Novoselov, the subject of water transport in 2D graphene-based nanocapillaries immediately attracted much attention [102,103]. GO is a single 2D lamellar nanomaterial with a large number of oxygen-containing functional groups such as carboxyl, hydroxyl, and epoxy groups which confer excellent hydrophilicity. Water molecules can flow frictionlessly in the sp^2 hybridized region on the surface of GO, and the GO nanosheets stacked on top of each other to form nanochannels can be used as water transport channels. Therefore, the introduction of GO into composite membranes can substantially improve the hydrophilicity and permeability of nanofiltration membranes. Nair et al. tested the water permeation behavior of GO membranes using an osmotic vaporization device [57]. It was found that the submicron-thick GO membranes were completely impermeable to most liquids, vapors, and gases, but allowed the unimpeded permeation of water. In addition, the free space of ≈4.6 Å between two graphene sheets in the GO membrane was sufficient to accommodate a layer of water, and it was these voids that formed a network of hydrophobic graphene nanocapillary tubes allowing for the frictionless flow of a single layer of water, thus enhancing water flux. Li et al. [103] embedded rGO-NH_2 in the polyamide layer of a nanofiltration membrane via interfacial polymerization to enhance the permeation performance of nanofiltration membranes. As the rGO-NH_2 content increased from 0 to 50 $mg \cdot L^{-1}$, the pure water flux increased from 30.44 $L \cdot m^{-2} \cdot h^{-1}$ to 38.57 $L \cdot m^{-2} \cdot h^{-1}$ at a pressure of 0.2 MPa.

Although GO-based membranes show great potential for water purification, the presence of multiple oxygen-containing functional groups leads to swelling of GO-based membranes during use and fouling of water molecules between the membranes leading to an enlargement of the mass transfer channels and a deterioration in solute retention. The ability to achieve different separation properties by adjusting the spacing between the layers of 2D materials is of great significance for the development and application of 2D

separation membranes in the field of accurate screening of ions/molecules in an aqueous solution. Therefore, most of the current research works have introduced functional groups that can participate in interfacial polymerization reactions to improve the compatibility of GO with the substrate, or embedded nanoparticles in the lamellae to increase the layer spacing to reduce the agglomeration phenomenon. Zhang et al. [104] reported for the first time that the layer spacing of GO membranes was efficiently regulated using soft particles–polyacrylonitrile gel particles (PAN GPs) as the intercalating agent. In addition, alkali treatment generated hydrophobic/hydrophilic structures on the surface of PAN GPs, which contributed to the dissolution–diffusion of water in the GO membrane. The GO membranes removed heavy metal complex ions Cu-EDTA^{2-} 4–13 times more efficiently than the 2D material NF membranes in the literature, reduced the water flux by only about 8% (from 15.9 to 14.6 L·h^{-1}) after 120 h of continuous filtration, and maintained a slightly higher retention rate in the permeate flux (from 96.4% to 99.2%). Chen et al. [105] immersed GO membranes in KCl solution, and the hydrated K^+ in the solution could be inserted into the refilled GO nanosheets which fixed the layer spacing to ≈11.4 Å. The swelling resistance of the nanofiltration membranes was also improved, suggesting that interactions within the 2D GO nanocapillary tubes were enhanced after the insertion of the hydrated K^+.

3.2. Conjugated Organic Skeleton

Recent studies have found that polymer porous substrates, which are usually only used to enhance the mechanical properties of graphene membranes, can also affect the separation properties of graphene membranes. For example, the size of the pores and the surface roughness of the substrate membrane can cause significant changes in the nanostructure of the graphene membrane loaded on it. Graphene membranes loaded on macroporous base membranes have greater water flux. However, if the pores of the basement membrane become too large, the soft graphene membrane is prone to collapse under high pressure, destabilizing the membrane. Inspired by "rebar" reinforced concrete, graphene membranes may also be stabilized by inserting stronger "rebar" COFs, which are porous crystalline materials with a periodic honeycomb network connected by covalent bonds. COFs with a two-dimensional structure are a class of crystalline porous materials connected by covalent bonds, with excellent properties such as a completely organic and metal-free skeleton, low mass density, good topology, structural diversity, good mechanical properties, and a hollow structure that can be used as an effective water channel. The first COF was synthesized by Yaghi et al. [106] in 2005 and, compared with conventional polymer and graphene materials, the 2D flat plate morphology of COF not only had a low density and large surface area, but also had tunable intrinsic pores that could be used as molecular transport channels [107,108]. From the perspective of membrane design, a 2D COF has the following characteristics. First, since the membrane separation process is mainly based on a size exclusion mechanism, the tunable pores of COFs can serve as selective molecular transport channels. Two-dimensional COFs have intrinsically well-defined and uniformly distributed pores to allow for the vertical transport of molecules through the laminar membrane. Second, a large number of 2D COFs exhibit good stability in aqueous or organic media due to strong covalent bonding [109,110]. In particular, imine-, hydrazine-, and ketamine-bonded COFs exhibit excellent stability in organic solvents [111]. Third, 2D COFs can be designed with tunable physicochemical properties by introducing different organized building blocks. Therefore, 2D COF can be used as an ideal membrane material, and efficient selective separation can be achieved by modifying 2D COF.

The two-dimensional lamellar structure of COF can be seamlessly integrated with graphene nanosheets to modulate the layer spacing between graphene sheets. By inserting COF into the lamellar structure composed of partially chemically reduced graphene oxide (prGO), Goh et al. [112] prepared high-performance composite nanofiltration membranes prGO/COF. By optimizing the incorporation of COF and the pore structure of the nylon-based membrane, the water flux of the prGO/COF membrane was increased by a factor of 27 over the prGO membrane without COF incorporation and without any decrease

in selectivity. In addition, the prGO/COF membrane also demonstrated a good self-supporting ability on the macroporous base membrane. By analyzing and calculating the membrane structure, the effective area of the prGO/COF membrane can be increased by 53.4%, and it can work continuously for more than 10 h while withstanding a deformation of 5 bar.

Shao et al. [113] proposed a one-step interfacial "molecular welding" strategy to synthesize COF nanofiltration membranes. Defect-free ultrathin COF nanofiltration membranes with precise screening ability were prepared by interfacial reaction synthesis using the coupled chemical environment of condensation polymerization of COF materials and self-polymerization of dopamine (DA), which was composed of 1, 3, 5-trimethylformylresorcinol (Tp) and p-phenylenediamine (Pa). The molecular flexibility of dopamine and the rigidity of the crystal structure of COFs endowed the polydopamine (PDA)/TpPa-COFs with unique structures and properties. Experimental results and density functional theory simulations revealed that the reactive radicals generated during the polymerization of dopamine facilitate nucleophilic reactions, which promoted the growth of COF thin layers while reducing their defects and regulating their pore sizes, and the COF nanofiltration membranes synthesized by the interfacial molecular welding method show an excellent "two-pronged" effect in desalination. The COF nanofiltration membranes synthesized by the interfacial molecular welding method showed excellent results in desalination, especially in the screening of monovalent/divalent ions.

To address the problems of poor stability and the trade-off relationship between permeability and selectivity of current GO membranes, Dong et al. [114] designed a stable and functionalized ceramic-based GOF nanofiltration membrane by inserting TU (thiourea) and MPD (m-phenylenediamine) molecules between the GO membrane layers to achieve covalent bonding cross-linking between GO nanosheets and form a more stable two-dimensional nano-passage. The salt retention rate of the TU-GOF membrane (GO/TU = 1:2) was significantly improved, Na_2SO_4 and $MgSO_4$ were almost completely retained, and the retention rates of NaCl (95.6 $\pm$ 1.14%) and $MgCl_2$ (90.2 $\pm$ 0.95%) were also higher than those reported for GO membranes, organic nanofiltration membranes, and emerging two-dimensional material membranes. When crosslinked with MPD molecules, the MPD-GOF membrane (GO/MPD = 1:4) achieved the simultaneous enhancement of retention and permeability for the four salts, overcoming the contradictory relationship between permeability and selectivity. The covalently cross-linked GOF membrane was used for the separation and removal of tetracycline (TC), oxytetracycline (OTC), chloramphenicol (CAP), and diclofenac sodium (DS) in water, and the results showed that the retention rate of CAP on the TU-GOF membrane was gradually increased with the increase in TU, and CAP could be almost completely removed when GO/TU was 1:3 (99.9 $\pm$ 0.1%). When GO/MPD was 1:6, the retention rate and water permeability of MPD-GOF membranes for CAP, DS, OTC, and TC increased simultaneously, realizing the rational size/chemistry regulation and enhanced stability of the nanochannels.

Wu et al. [115] proposed the use of an organic interlayer instead of an inorganic interlayer to optimize the structure of the porous matrix and manipulate the interfacial polymerization process. The PDA-COF hybrid organic interlayer was constructed on a PAN substrate by co-deposition of dopamine and COF nanosheets. The COF optimized the porous structure between the hybrid layers by physicochemical action to control the diffusion rate of monomers, and the PDA enhanced the interactions between the skin layer and the substrate, thus ensuring the stability of the membrane. The ultimately formed ultra-thin and dense PA layer, the thickness of which was drastically reduced from 79 nm to 11 nm, had a separation selectivity performance three times higher than that of a typical industrial filtration membrane. Zhu et al. [116] introduced the hydrophobic MOFs material, zeolite imidazolate backbone-8 (ZIF-8), modified by sodium polystyrene sulfonate into the active separation layer of a polypiperazine amide (PPA) nanofiltration membrane, and similarly obtained good results. When the mass fraction of modified ZIF-8 was 0.10%, the retention rate of the composite membrane for Na_2SO_4 was 93%, and the retention rate for

the reactive dyes reactive black 5 and reactive orchid 2 was greater than 99%; the membrane flux was increased from 10 $L \cdot m^{-2} \cdot h^{-1}$ without modified ZIF-8 to about 60 $L \cdot m^{-2} \cdot h^{-1}$.

Pang et al. [117] reported nano-sized UiO-66/GO sandwich membranes for water purification with hydrophilic MOF nanoparticles (UiO-66) used as microporous spacers. UiO-66 has a high porosity of ≈1200 $m^2 \cdot g^{-1}$ with a narrow and uniform 6.0 Å pore size, which is suitable for preventing hydrated Na^+ transport and reverse solute diffusion. In a cross-flow FO test at a pressure of 1 bar, the UiO-66/GO membrane had a fast water flux of 29.16 $L \cdot m^{-2} \cdot h^{-1}$, which was 270% higher than that of the pure GO membrane, while the reverse solute (NaCl) diffusion was reduced by 83.5%. Recently, Zhang et al. [118] reported a method to create composite MOF crystals with GO membranes. Instead of using MOF as a microporous spacer only, ZIF-8 nanocrystals were crystallized in situ at the edge of GO nanosheets to seal the relatively large inter-edge pores, which were replaced with the angstrom-sized pores in MOF. This particular composite membrane structure not only optimizes the inter-edge pores, but also enlarges the interlayer spacing, imparting mechanical integrity to the laminate framework thereby producing a stable microstructure. The modified nanofiltration membrane was capable of delivering 60 $L \cdot m^{-2} \cdot h^{-1} \cdot bar^{-1}$ (cross-flow) and the filtration system had near perfect methylene blue (MB) retention of ≈100% even after 180 h of operation under applied pressure (1 bar).

3.3. g-C_3N_4

Two-dimensional g-C_3N_4-based nanofiltration membranes are still a less developed area, and studies published to date have shown that 2D g-C_3N_4-based membranes have great potential for eliminating divalent ions and organic compounds. g-C_3N_4 is a material with a laminar structure, and the 3.11 Å regularly distributed triangular nanopores act as a water transport channel as well as molecular sieve functionality. Exfoliation provides g-C_3N_4 nanosheets with interlayer self-supporting spacers that are stable enough and stiff enough to resist swelling phenomena. Therefore, Chen et al. [119] modified polyamide nanofiltration membranes by incorporating g-C_3N_4 nanosheets, and the modified membranes had a water flux of 37.6 $L \cdot m^{-2} \cdot h^{-1}$ compared to the pristine membranes (20.9 $L \cdot m^{-2} \cdot h^{-1}$). Salt retention was 84% due to Donnan rejection effect and its good contamination resistance. Wang et al. [120] emphasized the function of nanofiltration membranes with g-C_3N_4 nanosheets to inhibit RB, EB, cytochromec, and gold nanoparticles, with water permeability of 27.5, 29.5, 28.6, and 30.8 $L \cdot m^{-2} \cdot h^{-1} \cdot bar^{-1}$, and retention of 75.5%, 87.2%, 93%, and 99.5% for the above pollutants, respectively. Wang et al. [121] also increased the water permeability (48 $L \cdot m^{-2} \cdot h^{-1} \cdot bar^{-1}$) while increasing the EB rejection rate to 97% by adding $Fe(OH)_3$ nanoparticles to g-C_3N_4 nanosheets.

Deep treatment of high-salt textile wastewater by fractionation of dye species and inorganic salts will contribute to sustainable resource recovery. This requires the removal of large amounts of inorganic salts from textile wastewater and the recovery of high purity dyes with better stability for reuse. Based on the surface cavities of bridging hydrolyzed polyacrylonitrile ultrafiltration membranes, Ye et al. [122] constructed high flux nanofiltration membranes using the biomimetic co-deposition of hydrophilic g-C_3N_4 nanosheets triggered by PDA/polyethylenimine with APS, which led to the effective separation of organics, dyes, and inorganic salts. When the concentration of g-C_3N_4 nanosheets was increased to 0.04%, the pore size of the ultrafiltration membrane was reduced to NF grade. As the g-C_3N_4 content increased, the pore size narrowed and the dye removal increased due to the size exclusion effect. However, the spatial effect had no effect on the salt retention because the g-C_3N_4 nanosheets were stacked onto the membrane surface, thereby allowing salt permeation, and a decrease in the retention of NaCl and Na_2SO_4 could be observed. The introduction of g-C_3N_4 nanosheets led to an improvement in the antifouling performance of the nanofiltration membranes, with a retention of organic dyes of 99.8% and an increase in water permeability of 28.4 $L \cdot m^{-2} \cdot h^{-1} \cdot bar^{-1}$. The retention of NaCl and Na_2SO_4 was very low, at 2.9% and 7.6%, respectively. Considering the excellent photocatalytic properties of g-C_3N_4 nanosheets, Li et al. [123] investigated the performance

of 2D g-C_3N_4-based photocatalytic membranes for the removal of inorganic salts. The generation of rGO was reduced by varying the irradiation time of the composite made of 2D GO and 2D g-C_3N_4 under UV light. This effect increased the retention of salts such as NaCl (67.5%), Na_2SO_4 (89.2%), $MgCl_2$ (24.2%), and $MgSO_4$ (40.7%), but resulted in a significant decrease in the permeability of the pure water from 16.4 to 2.0 $L{\cdot}m^{-2}{\cdot}h^{-1}{\cdot}bar^{-1}$ (UV irradiation reduced the hydrophilicity of the membrane). Despite the high retention of dye molecules and divalent ions by the g-C_3N_4 nanofiltration membrane, its water permeability remained relatively low. Therefore, improving the water permeability without sacrificing the retention rate is the direction of its development.

3.4. MXenes

Gogotsi et al. successfully stripped a series of 2D early transition metal carbides and nitrides (named MXenes) using hydrofluoric acid at room temperature in 2011 [124]. The general chemical formula of MXene is $M_{n+1}X_nT_x$ (n = 1, 2, or 3), where M stands for the early transition metal, X stands for C or N, and T stands for surface-terminated groups such as OH, O, and F. MXenes are attractive as membrane materials due to their tunable layer spacing, surface hydrophilicity, and high mechanical strength, and currently the most widely studied is $Ti_3C_2T_x$. However, unlike graphene materials and 2D COFs, exfoliation usually results in an uneven thickness of MXene nanosheets due to their covalently bonded lamellar structure, and MXene membranes also show higher stiffness than GO-based membranes. Although it was shown that MXene membranes constructed by simple filtration methods gave good results, an increase in permeability was often accompanied by a decrease in membrane selectivity. Moreover, turning MXene nanosheets into laminar membranes remains a challenging task [12,20,125]. Despite these problems, there have been several studies that have successfully applied MXene membranes to separation applications.

Most of the early studies focused on separations in aqueous media [59,126,127]. MXene membranes are hydrophilic, with a permeability greater than 1000 $L{\cdot}m^{-2}{\cdot}h^{-1}{\cdot}bar^{-1}$, while repelling molecules with hydrated sizes larger than their interlayer spacing with a high rejection rate (>2.5 nm) [31,59]. However, MXenes exhibit poor stability in the presence of oxygen and water [128,129]. Jung et al. [31] prepared 90 nm thick $Ti_3C_2T_x$-GO membranes by mixing GO with $Ti_3C_2T_x$ to study the dispersion of MXenes in various polar organic solvents. The dispersion of $Ti_3C_2T_x$ in N, N-dimethylformamide, N-methylpyrrolidone, dimethylsulfoxide, propylene carbonate, and ethanol, among other organic solvents, showed good dispersion stability. In addition, organic solvents slow down the degradation of $Ti_3C_2T_x$ compared to water, thus prolonging its service life. The effective layer spacing of the $Ti_3C_2T_x$-GO membranes is about 5 Å, corresponding to two layers of water molecules. During pressure-driven filtration at 5 bar, the composite membrane effectively retained dye molecules with hydration radii greater than 5 Å and positively charged dye molecules. The retention was 68% for methyl red, 99.5% for methylene blue, 93.5% for rose red, and 100% for brilliant blue (hydration radii of 4.87, 5.04, 5.88, and 7.98 Å, respectively). Similar to GO membranes, the interlayer spacing of MXene membranes acts as a transport channel for molecules. Therefore, regulating the interlayer spacing is important for the permeability of MXene membranes. Recently, Wu et al. [34] modulated the surface wettability by chemically grafting a hydrophilic group (-NH_2) or hydrophobic groups (-C_6H_5, -$C_{12}H_{25}$) to drastically increase the speed of polar molecules moving through hydrophilic nano-channels. Ultimately, ultra-high permeability at high capillary pressures of 3337 $L{\cdot}m^{-2}{\cdot}h^{-1}{\cdot}bar^{-1}$ for acetonitrile and 3018 $L{\cdot}m^{-2}{\cdot}h^{-1}{\cdot}bar^{-1}$ for methanol was achieved for precise screening separation.

4. Stability–Antifouling Properties of 2D Material NF Membrane

Membrane fouling is an unavoidable problem in the actual use of NF membranes. The membrane antifouling property is another factor that is very important in evaluating an NF membrane's performance. The performance reduction, increase in energy consumption, and service life shortening caused by membrane fouling will greatly increase the cost of NF

technology and limit the application potential of NF membranes. The incorporation of 2D materials into NF membranes has demonstrated better resistance towards fouling accompanied by improved separation properties. Bi et al. [130] constructed a fouling-resistant nanofiltration membrane by introducing graphite quantum dots into the polyamide separation layer, and the modified nanofiltration membrane achieved flux recoveries of up to 91.85%, 99.06%, and 65.26% for BSA, HA, and emulsified oils, respectively, when the amount of graphite quantum dots added was 0.2%. The antifouling ability of MOF-based NF membranes is also a critical area of research.

CNTs and GO especially have shown promising results in enhancing the antifouling performance of nanofiltration membranes. Long et al. [131] have investigated the use of CNT-interlayered NF membranes to enhance the antifouling performance. The inclusion of a CNT interlayer reduced membrane fouling and enhanced the fouling reversibility, which could be attributed to its more uniform water flux distribution. This study also demonstrated the potential trade-off between increasing the thickness of the CNT interlayer to facilitate water transport and its impact on hydraulic resistance. Safarpour et al. [132] introduced TiO_2-loaded reduced GO (rGO/TiO_2) into polyamide membranes prepared by interfacial polymerization of piperazine and homotrimethylene tricarbonyl chloride to improve membrane fouling resistance, and the contact angle of the membranes decreased from 67.0° before the addition of rGO/TiO_2 to 47.2° at an addition level of 0.02% and the flux increased from 48.3 $L{\cdot}m^{-2}{\cdot}h^{-1}$ to 61.1 $L{\cdot}m^{-2}{\cdot}h^{-1}$. The amount of adsorbed BSA on the rGO/TiO_2/NF membrane decreased by about 1.5–3.0 times compared with that on the bare NF membrane. Furthermore, a lower flux loss rate was observed in the modified membranes, confirming the enhanced fouling resistance ability of the bare NF membrane through the incorporation of rGO/TiO_2. Abdi et al. [133] prepared magnetic GO-based composites (MMGO) by chemically bonding bisguanidine onto the surface of graphene in conjunction with magnetic iron oxides, and finally blended with PES to make the membranes. The introduction of MMGO resulted in increased membrane flux and flux recovery. With powdered milk solution (8000 ppm) as the model foulant, the flux recovery rate of the pure PES membrane without added particles was 48.7%, while the flux recovery rate increased to 90.6% with the addition of 0.5% MMGO. Meng et al. [134] constructed a contamination-resistant nano-filtration membrane by using brominated polyphenylene ether (BPPO) as the support layer and layer-by-layer self-assembled GO, and ethylenediamine (EDA) was used as the cross-linking agent, which formed a chemical bond between the layers and the graphene with the basement membrane in order to enhance the stability of the membrane. The chemical bond was formed between the layers and between graphene and the base membrane to enhance the stability of the membrane. The results showed that the BPPO/EDA/GO membrane still had a good flux and desalination rate after 1 month of immersion in water. The introduction of GO, triethylenetetramine (TETA), and $CuFe_2O_4$ into PES NF membranes enhanced the removal rates for arsenic and total dissolved solids in wastewater treatment. The presence of $–NH_2$ and –COOH functional groups on the membrane surface introduced by TETA and GO contributed to the excellent hydrophilicity of GO-TETA-$CuFe_2O_4$ (39.88°). GO-TETA-$CuFe_2O_4$ membranes demonstrated significantly higher resistance to fouling than the PES NF membranes. The hydraulic reversibility test showed that the total resistance changes from 6.78×10^{12} m^{-1} to 2.07×10^{12} m^{-1} [135].

Hydrophilicity plays a crucial role in membrane applications by allowing water molecules to diffuse quickly through the membrane and reducing surface contamination [136]. Abdikheibari et al. [137] have delved into the fabrication of NF membranes through the incorporation of amine functionalized-boron nitride ($BN(NH_2)$) nanosheets to enhance fouling resistance. The PPA membrane containing 0.004 wt% of $BN(NH_2)$ nanosheets (PPA-BN-4) exhibited a more negatively charged and hydrophilic surface compared with the bare PPA membrane. The normalized flux remained at 0.97 during the filtration of moderately-concentrated HA solutions, which confirmed the excellent fouling resistance behavior of the PPA-BN-4 membrane. Since the nitrogen atoms of g-C_3N_4 form

hydrogen bonds with water molecules [138], it was possible to improve the wettability of the membrane, thus improving the hydrophilicity and water flux. Therefore, g-C_3N_4 showed the potential to reduce membrane contamination [122]. However, it is worth noting that the configurations of g-C_3N_4 have effect on the diffusion behaviors of water. Molecular dynamics simulation results indicated that pure water flow was slower in pristine g-C_3N_4 confinement compared to that in benzene ring-doped g-C_3N_4 [139].

Overall, the incorporation of 2D materials has shown significant promise in improving the antifouling performance of nanofiltration membranes. These advancements underscore the growing potential for the development of highly efficient and sustainable membrane technologies.

5. Conclusions

Nanofiltration technology is a green and durable water treatment technology with nano-level retention of substances; it is widely used in the field of water treatment, and can solve the problems associated with drinking water, industrial wastewater, and other areas of metal ion water pollution. Improving the selective separability and application stability of NF membranes is an inevitable requirement for the long-term promotion and application of NF membranes. Two-dimensional material NF membranes have high selectivity and permeability. At present, 2D material-based NF membranes still have deficiencies, most of the NF membrane modification methods have complex processes, and there are also some membrane modification modifiers with high costs, which are not suitable for large-scale popularization and application. The functionalized modification of 2D materials in the field of organic system separation membrane preparation shows a good application potential, but the relevant research is still insufficient. The molecular design of 2D materials for directional modification, in order to expand their application in the process of organic solvent system membrane separation, is a potential research direction to lay the foundations for the preparation of high-performance, high-stability NF membrane. In conclusion, the modification of NF membranes still needs to be further explored; with the continuous deepening of the research and references to the results of other related disciplines, the application of NF membranes will become broader.

Author Contributions: Data collection, S.X.; writing—original draft preparation, S.X., S.D., X.Q. and Y.H.; writing—review and editing, S.X. and M.S.; supervision, M.S. All authors have read and agreed to the published version of the manuscript.

Funding: This research received no external funding.

Conflicts of Interest: Author Sichu Xing was employed by Shanghai Municipal Engineering Design Institute (Group) Co., Ltd. The remaining authors declare that the research was conducted in the absence of any commercial or financial relationships that could be construed as a potential conflict of interest.

References

1. Liyanage, C.P.; Yamada, K. Impact of population growth on the water quality of natural water bodies. *Sustainability* **2017**, *9*, 1405. [CrossRef]
2. Sholl, D.S.; Lively, R. Seven chemical separations to change the world. *Nature* **2016**, *532*, 435–437. [CrossRef] [PubMed]
3. Mauter, M.; Zucker, I.; Perreault, F.; Werber, J.; Kim, J.; Elimelech, M. The role of nanotechnology in tackling global water challenges. *Nat. Sustain.* **2018**, *1*, 166–175. [CrossRef]
4. Elimelech, M.; Phillip, W. The future of seawater desalination: Energy, technology, and the environment. *Science* **2011**, *333*, 712–717. [CrossRef]
5. Shannon, M.; Bohn, P.; Elimelech, M.; Georgiadis, J.; Mariñas, B.; Mayes, A. Science and technology for water purification in the coming decades. *Nature* **2008**, *452*, 301–310. [CrossRef]
6. Wang, K.; Wang, X.; Januszewski, B.; Liu, Y.; Li, D.; Elimelech, M.; Huang, X. Tailored design of nanofiltration membranes for water treatment based on synthesis-property-performance relationships. *Chem. Soc. Rev.* **2022**, *51*, 672–719. [CrossRef]
7. Balamurugan, R.; Sundarrajan, S.; Ramakrishna, S. Recent trends in nanofibrous membranes and their suitability for air and water filtrations. *Membranes* **2011**, *1*, 232–248. [CrossRef]
8. Zhou, H.; Jin, W. Membranes with intrinsic micro-porosity: Structure, solubility, and applications. *Membranes* **2019**, *9*, 3. [CrossRef]

9. Shahkaramipour, N.; Tran, T.N.; Ramanan, S.; Lin, H. Membranes with surface-enhanced antifouling properties for water purification. *Membranes* **2017**, *7*, 13. [CrossRef]
10. Ursino, C.; Castro-Muñoz, R.; Drioli, E.; Gzara, L.; Albeirutty, M.; Figoli, A. Progress of nanocomposite membranes for water treatment. *Membranes* **2018**, *8*, 18. [CrossRef]
11. Verliefde, A.; Cornelissen, E.; Heijman, S.; Verberk, J.; Amy, G.; Bruggen, B.; Dijk, J. The role of electrostatic interactions on the rejection of organic solutes in aqueous solutions with nanofiltration. *J. Membr. Sci.* **2008**, *322*, 52–66. [CrossRef]
12. Li, Y.; Wang, X.; Xi, W.; Zheng, Z.; Zhao, J. LBL assembled graphene oxide-based nanofiltration membranes with tunable surface charges and high selectivity for charged organic dye molecules. *Mater. Lett.* **2023**, *341*, 134289. [CrossRef]
13. Suhalim, N.; Kasim, N.; Mahmoudi, E.; Shamsudin, I.; Mohammad, A.; Mohamed Zuki, F.; Jamari, N. Rejection mechanism of ionic solute removal by nanofiltration membranes: An overview. *Nanomaterials* **2022**, *12*, 437. [CrossRef]
14. Haemers, J.; Saadaoui, H.; Jourdain, S.; Falcinelli, U. In situ thermal treatment in urban polluted areas: Application of thermopile. In Proceedings of the 10th ConSoil Conference, Milan, Italy, 3–6 June 2008.
15. Truex, M.; Gillie, J.; Powers, J.; Lynch, K. Assessment of in situ thermal treatment for chlorinated organic source zones. *Remediation* **2009**, *19*, 7–17. [CrossRef]
16. Park, H.; Kamcev, J.; Robeson, L.; Elimelech, M.; Freeman, B. Maximizing the right stuff: The trade-off between membrane permeability and selectivity. *Science* **2017**, *356*, eaab0530. [CrossRef]
17. Zhang, R.; Tian, J.; Gao, S.; Bruggen, B. How to coordinate the trade-off between water permeability and salt rejection in nanofiltration? *J. Mater. Chem. A* **2020**, *8*, 8831–8847. [CrossRef]
18. Zhang, H.; He, Q.; Luo, J.; Wan, Y.; Darling, S. Sharpening nanofiltration: Strategies for enhanced membrane selectivity. *ACS Appl. Mater. Interfaces* **2020**, *12*, 39948–39966. [CrossRef]
19. Guo, S.; Wan, Y.; Chen, X.; Luo, J. Loose nanofiltration membrane custom-tailored for resource recovery. *Chem. Eng. J.* **2021**, *409*, 127376. [CrossRef]
20. Liu, P.; Hou, J.; Zhang, Y.; Li, L.; Lu, X.; Tang, Z. Two-dimensional material membranes for critical separations. *Inorg. Chem. Front.* **2020**, *7*, 2560–2581. [CrossRef]
21. Kim, S.; Wang, H.; Lee, Y.M. 2D nanosheets and their composite membranes for water, gas, and ion separation. *Angew. Chem. Int. Edit.* **2019**, *131*, 17674–17689. [CrossRef]
22. Kang, Y.; Xia, Y.; Wang, H.; Zhang, X. 2D laminar membranes for selective water and ion transport. *Adv. Funct. Mater.* **2019**, *29*, 1902014. [CrossRef]
23. Wang, J.; Chen, P.; Shi, B.; Guo, W.; Jaroniec, M.; Qiao, S. A regularly channeled lamellar membrane for unparalleled water and organics permeation. *Angew. Chem. Int. Edit.* **2018**, *57*, 6814–6818. [CrossRef] [PubMed]
24. Huang, L.; Chen, J.; Gao, T.; Zhang, M.; Li, Y.; Dai, L.; Qu, L.; Shi, G. Reduced graphene oxide membranes for ultrafast organic solvent nanofiltration. *Adv. Mater.* **2016**, *28*, 8669–8674. [CrossRef] [PubMed]
25. Yang, Q.; Su, Y.; Chi, C.; Cherian, C.; Huang, K.; Kravets, V.; Wang, F.; Zhang, J.; Pratt, A.; Grigorenko, A.; et al. Ultrathin graphene-based membrane with precise molecular sieving and ultrafast solvent permeation. *Nat. Mater.* **2017**, *16*, 1198–1202. [CrossRef]
26. Gao, T.; Wu, H.; Tao, L.; Qu, L.; Li, C. Enhanced stability and separation efficiency of graphene oxide membranes in organic solvent nanofiltration. *J. Mater. Chem. A* **2018**, *6*, 19563–19569. [CrossRef]
27. Wang, S.; Mahalingam, D.; Sutisna, B.; Nunes, S. 2D-dual-spacing channel membranes for high performance organic solvent nanofiltration. *J. Mater. Chem. A* **2019**, *7*, 11673–11682. [CrossRef]
28. Kandambeth, S.; Biswal, B.; Chaudhari, H.; Rout, K.; Kunjattu, H.; Mitra, S.; Karak, S.; Das, A.; Mukherjee, R.; Kharul, U.; et al. Selective molecular sieving in self-standing porous covalent-organic-framework membranes. *Adv. Mater.* **2017**, *29*, 1603945. [CrossRef]
29. Dey, K.; Pal, M.; Rout, K.; Kunjattu, H.; Das, A.; Mukherjee, R.; Kharul, U.; Banerjee, R. Selective molecular separation by interfacially crystallized covalent organic framework thin films. *J. Am. Chem. Soc.* **2017**, *139*, 13083–13091. [CrossRef]
30. Shinde, D.B.; Sheng, G.; Li, X.; Ostwal, M.; Emwas, A.; Huang, K.; Lai, Z. Crystalline 2D covalent organic framework membranes for high-flux organic solvent nanofiltration. *J. Am. Chem. Soc.* **2018**, *140*, 14342–14349. [CrossRef]
31. Kang, K.; Kim, D.; Ren, C.; Cho, K.; Kim, S.; Choi, J.; Nam, Y.; Gogotsi, Y.; Jung, H. Selective molecular separation on $Ti_3C_2T_x$–graphene oxide membranes during pressure-driven Filtration: Comparison with graphene oxide and MXenes. *ACS Appl. Mater. Interfaces* **2017**, *9*, 44687–44694. [CrossRef]
32. Halder, A.; Karak, S.; Addicoat, M.; Bera, S.; Chakraborty, A.; Kunjattu, S.; Pachfule, P.; Heine, T.; Banerjee, R. Ultrastable imine-based covalent organic frameworks for sulfuric acid recovery: An effect of interlayer hydrogen bonding. *Angew. Chem. Int. Edit.* **2018**, *57*, 5797–5802. [CrossRef] [PubMed]
33. Dey, K.; Kunjattu, H.S.; Chahande, A.; Banerjee, R. Nanoparticle size-fractionation through self-standing porous covalent organic framework films. *Angew. Chem. Int. Edit.* **2020**, *59*, 1161–1165. [CrossRef] [PubMed]
34. Wu, X.; Cui, X.; Wu, W.; Wang, J.; Li, Y.; Jiang, Z. Elucidating ultrafast molecular permeation through well-defined 2D nanochannels of lamellar membranes. *Angew. Chem. Int. Edit.* **2019**, *58*, 18524–18529. [CrossRef] [PubMed]
35. Liu, G.; Jin, W.; Xu, N. Two-dimensional-material membranes: A new family of high-performance separation membranes. *Angew. Chem. Int. Edit.* **2016**, *55*, 13384–13397. [CrossRef]

36. Zhu, J.; Hou, J.; Uliana, A.; Zhang, Y.; Tian, M.; Bruggen, B. The rapid emergence of two-dimensional nanomaterials for high-performance separation membranes. *J. Mater. Chem. A* **2018**, *6*, 3773–3792. [CrossRef]
37. Cai, X.; Luo, Y.; Liu, B.; Cheng, H. Preparation of 2D material dispersions and their applications. *Chem. Soc. Rev.* **2018**, *47*, 6224–6266. [CrossRef] [PubMed]
38. Zhao, Y.; Xie, Y.; Liu, Z.; Wang, X.; Chai, Y.; Yan, F. Two-dimensional material membranes: An emerging platform for controllable mass transport applications. *Small* **2014**, *10*, 4521–4542. [CrossRef] [PubMed]
39. Moghadam, F.; Park, H.B. 2D nanoporous materials: Membrane platform for gas and liquid separations. *2D Mater.* **2019**, *6*, 042002. [CrossRef]
40. Song, N.; Gao, X.; Ma, Z.; Wang, X.; Wei, Y.; Gao, C. A review of graphene-based separation membrane: Materials, characteristics, preparation and applications. *Desalination* **2018**, *437*, 59–72. [CrossRef]
41. Lian, B.; Deng, J.; Leslie, G.; Bustamante, H.; Sahajwalla, V.; Nishina, Y.; Joshi, R. Surfactant modified graphene oxide laminates for filtration. *Carbon* **2017**, *116*, 240–245. [CrossRef]
42. Wang, Q.; Aubry, C.; Chen, Y.; Song, H.; Zou, L. Insights on tuning the nanostructure of rGO laminate membranes for low pressure osmosis process. *ACS Appl. Mater. Interfaces* **2017**, *9*, 22509–22517. [CrossRef] [PubMed]
43. Hong, S.; Zou, G.; Kim, H.; Huang, D.; Wang, P.; Alshareef, H. Photothermoelectric response of $Ti_3C_2T_x$ MXene confined ion channels. *ACS Nano* **2020**, *14*, 9042–9049. [CrossRef]
44. Zhao, M.; Lu, Q.; Ma, Q.; Zhang, H. Two-dimensional metal-organic framework nanosheets. *Small Methods* **2017**, *1*, 1600030. [CrossRef]
45. Yan, P.; Ji, L.; Liu, X.; Guan, Q.; Guo, J.; Shen, Y.; Zhang, H.; Wei, W.; Cui, X.; Xu, Q. 2D amorphous-MoO_{3-x}@ Ti_3C_2-MXene non-van der Waals heterostructures as anode materials for lithium-ion batteries. *Nano Energy* **2021**, *86*, 106139. [CrossRef]
46. Liu, G.; Jin, W.; Xu, N. Graphene-based membranes. *Chem. Soc. Rev.* **2015**, *44*, 5016–5030. [CrossRef] [PubMed]
47. Wang, Z.; Yu, H.; Xia, J.; Zhang, F.; Li, F.; Xia, Y.; Li, Y. Novel GO-blended PVDF ultrafiltration membranes. *Desalination* **2012**, *299*, 50–54. [CrossRef]
48. Zhang, X.; Liu, Y.; Sun, C.; Ji, H.; Zhao, W.; Sun, S.; Zhao, C. Graphene oxide-based polymeric membranes for broad water pollutant removal. *RSC Adv.* **2015**, *5*, 100651–100662. [CrossRef]
49. Zinadini, S.; Zinatizadeh, A.A.; Rahimi, M.; Vatanpour, V.; Zangeneh, H. Preparation of a novel antifouling mixed matrix PES membrane by embedding graphene oxide nanoplates. *J. Membr. Sci.* **2014**, *453*, 292–301. [CrossRef]
50. Tang, C.; Zulhairun, A.; Wong, T.; Alireza, S.; Marzuki, M.; Ismail, A. Water transport properties of boron nitride nanosheets mixed matrix membranes for humic acid removal. *Heliyon* **2019**, *5*, e01142. [CrossRef]
51. Cao, K.; Jiang, Z.; Zhao, J.; Zhao, C.; Gao, C.; Pan, F.; Wang, B.; Cao, X.; Yang, J. Enhanced water permeation through sodium alginate membranes by incorporating graphene oxides. *J. Membr. Sci.* **2014**, *469*, 272–283. [CrossRef]
52. He, L.; Dumée, L.F.; Feng, C.; Velleman, L.; Reis, R.; She, F.; Gao, W.; Kong, L. Promoted water transport across graphene oxide-poly (amide) thin film composite membranes and their antibacterial activity. *Desalination* **2015**, *365*, 126–135. [CrossRef]
53. Ganesh, B.; Isloor, A.M.; Ismail, A.F. Enhanced hydrophilicity and salt rejection study of graphene oxide-polysulfone mixed matrix membrane. *Desalination* **2013**, *313*, 199–207. [CrossRef]
54. Liu, Y. Beyond graphene oxides: Emerging 2D molecular sieve membranes for efficient separation. *Chin. J. Chem. Eng.* **2019**, *27*, 1257–1271. [CrossRef]
55. Qiu, L.; Zhang, X.; Yang, W.; Wang, Y.; Simon, G.P.; Li, D. Controllable corrugation of chemically converted graphene sheets in water and potential application for nanofiltration. *Chem. Commun.* **2011**, *47*, 5810–5812. [CrossRef] [PubMed]
56. Huang, H.; Song, Z.; Wei, N.; Shi, L.; Mao, Y.Y.; Ying, Y.L.; Sun, L.W.; Xu, Z.P.; Peng, X.S. Ultrafast viscous water flow through nanostrand-channelled graphene oxide membranes. *Nat. Commun.* **2013**, *4*, 2979. [CrossRef] [PubMed]
57. Nair, R.; Wu, H.; Jayaram, P.; Grigorieva, I.; Geim, A. Unimpeded permeation of water through helium-leak-tight graphene-based membranes. *Science* **2012**, *335*, 442–444. [CrossRef] [PubMed]
58. Huang, K.; Liu, G.; Shen, J.; Chu, Z.; Zhou, H.; Gu, X.; Jin, W.; Xu, N. High-efficiency water-transport channels using the synergistic effect of a hydrophilic polymer and grapheneoxide laminates. *Adv. Funct. Mater.* **2015**, *25*, 5809–5815. [CrossRef]
59. Ren, C.; Alhabeb, M.; Byles, B.; Zhao, M.; Anasori, B.; Pomerantseva, E.; Mahmoud, K.; Gogotsi, Y. Voltage-gated ions sieving through 2D MXene $Ti_3C_2T_x$ membranes. *ACS Appl. Nano Mater.* **2018**, *1*, 3644–3652. [CrossRef]
60. Liu, T.; Tian, L.; Graham, N.; Yang, B.; Yu, W.; Sun, K. Regulating the interlayer spacing of graphene oxide membranes and enhancing their stability by use of PACl. *Environ. Sci. Technol.* **2019**, *53*, 11949–11959. [CrossRef]
61. Ren, C.; Hatzell, K.; Alhabeb, M.; Ling, Z.; Mahmoud, K.; Gogotsi, Y. Charge-and size-selective ion sieving through $Ti_3C_2T_x$ MXene membranes. *J. Phys. Chem. Lett.* **2015**, *6*, 4026–4031. [CrossRef]
62. Ding, L.; Li, L.; Liu, Y.; Wu, Y.; Lu, Z.; Deng, J.; Wei, Y.; Caro, J.; Wang, H. Effective ion sieving with $Ti_3C_2T_x$ MXene membranes for production of drinking water from seawater. *Nat. Sustain.* **2020**, *3*, 296–302. [CrossRef]
63. Hirunpinyopas, W.; Prestat, E.; Worrall, S.D.; Haigh, S.J.; Dryfe, R.A.; Bissett, M.A. Desalination and nanofiltration through functionalized laminar MoS_2 membranes. *ACS Nano* **2017**, *11*, 11082–11090. [CrossRef] [PubMed]
64. Mi, B. Graphene oxide membranes for ionic and molecular sieving. *Science* **2014**, *343*, 740–742. [CrossRef] [PubMed]
65. Zhang, Z.H.; Liang, Z.H.; Guo, Z.C.; Gui, X.Y.; Junaid, M.; Zhao, Z.; Ma, J.Y.; Fang, Z.H.; Mo, D.; Duan, J.L.; et al. Construction of bifunctional vertical nanochannels in GOM with swift heavy ion irradiation for enhancing the stability and nanofiltration performance. *Sep. Purif. Technol.* **2023**, *322*, 124271. [CrossRef]

66. Shevate, R.; Shaffer, D.L. Large-area 2D covalent organic framework membranes with tunable single-digit nanopores for predictable mass transport. *ACS Nano.* **2022**, *16*, 2407–2418. [CrossRef] [PubMed]
67. Liu, X.; Zhang, L.; Cui, X.; Zhang, Q.; Hu, W.; Du, J.; Zeng, H.; Xu, Q. 2D material nanofiltration membranes: From fundamental understandings to rational design. *Adv. Sci.* **2021**, *8*, 2102493. [CrossRef]
68. Cheng, L.; Liu, G.; Zhao, J.; Jin, W. Two-dimensional-material membranes: Manipulating the transport pathway for molecular separation. *Acc. Mater. Res.* **2021**, *2*, 114–128. [CrossRef]
69. Wu, Y.; Li, D.; Wu, C.; Hwang, H.; Cui, Y. Electrostatic gating and intercalation in 2D materials. *Nat. Rev. Mater.* **2023**, *8*, 41–53. [CrossRef]
70. Yadav, D.; Hazarika, S.; Ingole, P. Recent development in nanofiltration (NF) membranes and their diversified applications. *Emergent Mater.* **2021**, *5*, 1311–1328. [CrossRef]
71. Razmjou, A.; Asadnia, M.; Hosseini, E.; Korayem, A.H.; Chen, V. Design principles of ion selective nanostructured membranes for the extraction of lithium ions. *Nat. Commun.* **2019**, *10*, 5793. [CrossRef]
72. David, C.; Grossman, J. Nanoporous graphene as a reverse osmosis membrane: Recent insights from theory and simulation. *Desalination* **2015**, *366*, 59–70.
73. Alhabeb, M.; Maleski, K.; Anasori, B.; Lelyukh, P.; Clark, L.; Sin, S.; Gogotsi, Y. Guidelines for synthesis and processing of two-dimensional titanium carbide ($Ti_3C_2T_x$ MXene). *Chem. Mater.* **2017**, *29*, 7633–7644. [CrossRef]
74. Mahmood, J.; Lee, E.; Jung, M.; Shin, D.; Jeon, I.; Jung, S.M.; Choi, H.J.; Seo, J.M.; Bae, S.Y.; Sohn, S.D.; et al. Nitrogenated holey two-dimensional structures. *Nat. Commun.* **2015**, *6*, 6486. [CrossRef] [PubMed]
75. Chi, M.Z.; Zheng, P.Y.; Wei, M.X.; Zhu, A.M.; Zhong, L.B.; Zhang, Q.G.; Liu, Q.L. Polyamide composite nanofiltration membrane modified by nanoporous TiO_2 interlayer for enhanced water permeability. *J. Ind. Eng. Chem.* **2022**, *115*, 230–240. [CrossRef]
76. Kang, J.; Choi, Y.; Kim, J.H.; Choi, E.; Choi, S.E.; Kwon, O.; Kim, D.W. Functionalized nanoporous graphene membrane with ultrafast and stable nanofiltration. *J. Membr. Sci.* **2021**, *618*, 118635. [CrossRef]
77. Li, Y.; Wu, Q.X.; Guo, X.H.; Zhang, M.C.; Chen, B.; Wei, G.Y.; Li, X.; Li, X.F.; Li, S.J.; Ma, L.J. Laminated self-standing covalent organic framework membrane with uniformly distributed subnanopores for ionic and molecular sieving. *Nat. Commun.* **2020**, *11*, 599. [CrossRef] [PubMed]
78. Kim, C.; Koh, D.Y.; Lee, Y.; Choi, J.; Cho, H.S.; Choi, M. Bottom-up synthesis of two-dimensional carbon with vertically aligned ordered micropores for ultrafast nanofiltration. *Sci. Adv.* **2023**, *9*, eade7871. [CrossRef] [PubMed]
79. Zhao, X.T.; Sun, J.S.; Cheng, X.H.; Qiu, Q.Q.; Ma, G.M.; Jiang, C.Y.; Pan, J.F. Colloidal 2D covalent organic framework-tailored nanofiltration membranes for precise molecular sieving. *ACS Appl. Mater. Interfaces* **2023**, *15*, 53924–53934. [CrossRef] [PubMed]
80. Li, J.; Cheng, L.; Song, W.; Xu, Y.; Liu, F.; Wang, Z. In-situ sol-gel generation of SiO_2 nanoparticles inside polyamide membrane for enhanced nanofiltration. *Desalination* **2022**, *540*, 115981. [CrossRef]
81. Ritt, C.; Werber, J.; Wang, M.; Elimelech, M. Ionization behavior of nanoporous polyamide membranes. *Proc. Natl. Acad. Sci. USA* **2020**, *117*, 30191–30200. [CrossRef]
82. Vatanpour, V.; Keskin, B.; Mehrabani, S.; Karimi, H.; Arabi, N.; Behroozi, A.; Shokrollahi-far, A.; Gul, B.; Koyuncu, I. Investigation of boron nitride/silver/graphene oxide nanocomposite on separation and antibacterial improvement of polyethersulfone membranes in wastewater treatment. *J. Environ. Chem. Eng.* **2022**, *10*, 107035. [CrossRef]
83. Li, Y.; Yang, S.; Zhang, K.; Bruggen, B. Thin film nanocomposite reverse osmosis membrane modified by two dimensional laminar MoS_2 with improved desalination performance and fouling-resistant characteristics. *Desalination* **2019**, *454*, 48–58. [CrossRef]
84. Tsou, C.; An, Q.; Lo, S.; Guzman, M.; Hung, W.; Hu, C.; Lee, K.; Lai, J. Effect of microstructure of graphene oxide fabricated through different self-assembly techniques on 1-butanol dehydration. *J. Membr. Sci.* **2015**, *477*, 93–100. [CrossRef]
85. Guo, B.; Jiang, S.; Tang, M.; Li, K.; Sun, S.; Chen, P.; Zhang, S. MoS_2 membranes for organic solvent nanofiltration, stability and structural control. *J. Phys. Chem. Lett.* **2019**, *10*, 4609–4617. [CrossRef] [PubMed]
86. Hu, M.; Mi, B. Enabling graphene oxide nanosheets as water separation membranes. *Environ. Sci. Technol.* **2013**, *47*, 3715–3723. [CrossRef]
87. Kang, Z.; Peng, Y.; Hu, Z.; Qian, Y.; Chi, C.; Yeo, L.; Tee, L.; Zhao, D. Mixed matrix membranes composed of two-dimensional metal–organic framework nanosheets for pre-combustion CO_2 capture: A relationship study of filler morphology versus membrane performance. *J. Mater. Chem. A* **2015**, *3*, 20801–20810. [CrossRef]
88. Jiang, S.; Koh, A.; Chong, K.; Zhang, S. Opening organic solvent pathways by molybdenum disulfide in mixed matrix membranes for molecular separation. *J. Membr. Sci.* **2019**, *585*, 60–66. [CrossRef]
89. Wang, C.; Park, M.J.; Yu, H.; Matsuyama, H.; Drioli, E.; Shon, H.K. Recent advances of nanocomposite membranes using layer-by-layer assembly. *J. Membr. Sci.* **2022**, *661*, 120926. [CrossRef]
90. Yang, Y.; Goh, K.; Wang, R.; Bae, T. High-performance nanocomposite membranes realized by efficient molecular sieving with CuBDC nanosheets. *Chem. Commun.* **2017**, *53*, 4254–4257. [CrossRef]
91. Sun, P.; Zhu, M.; Wang, K.; Zhong, M.; Wei, J.; Wu, D.; Xu, Z.; Zhu, H. Selective ion penetration of graphene oxide membranes. *ACS Nano* **2013**, *7*, 428–437. [CrossRef]
92. Lou, Y.; Liu, G.; Liu, S.; Shen, J.; Jin, W. A facile way to prepare ceramic-supported graphene oxide composite membrane via silane-graft modification. *Appl. Surf. Sci.* **2014**, *307*, 631–637. [CrossRef]

93. Wang, L.; Boutilier, M.S.; Kidambi, P.R.; Jang, D.; Hadjiconstantinou, N.; Karnik, R. Fundamental transport mechanisms, fabrication and potential applications of nanoporous atomically thin membranes. *Nat. Nanotechnol.* **2017**, *12*, 509–522. [CrossRef] [PubMed]
94. Celebi, K.; Buchheim, J.; Wyss, R.M.; Droudian, A.; Gasser, P.; Shorubalko, I.; Kye, J.; Lee, C.; Park, H. Ultimate permeation across atomically thin porous graphene. *Science* **2014**, *344*, 289–292. [CrossRef] [PubMed]
95. Wyss, R.M.; Tian, T.; Yazda, K.; Park, H.; Shih, C. Macroscopic salt rejection through electrostatically gated nanoporous graphene. *Nano Lett.* **2019**, *19*, 6400–6409. [CrossRef] [PubMed]
96. Yang, Y.; Yang, X.; Liang, L. Large-area graphene-nanomesh/carbon-nanotube hybrid membranes for ionic and molecular nanofiltration. *Science* **2019**, *364*, 1057–1062. [CrossRef] [PubMed]
97. Prozorovska, L.; Kidambi, P.R. State-of-the-Art and Future Prospects for atomically thin membranes from 2D materials. *Adv. Mater.* **2018**, *30*, 1801179. [CrossRef] [PubMed]
98. Heiranian, M.; Farimani, A.; Aluru, N. Water desalination with a single-layer MoS_2 nanopore. *Nat. Commun.* **2015**, *6*, 8616. [CrossRef] [PubMed]
99. Thiruraman, J.; Masih Das, P.; Drndic, M. Stochastic Ionic transport in single atomic zero-dimensional pores. *ACS Nano* **2020**, *14*, 11831–11845. [CrossRef] [PubMed]
100. Culp, T.; Khara, B.; Brickey, K.; Geitner, M.; Zimudzi, T.; Wilbur, J.; Jons, S.; Roy, A.; Paul, M.; Ganapathysubramanian, B.; et al. Nanoscale control of internal inhomogeneity enhances water transport in desalination membranes. *Science* **2021**, *371*, 72–75. [CrossRef]
101. Geim, A.; Novoselov, K. The rise of graphene. *Nat. Mater.* **2007**, *6*, 183–191. [CrossRef]
102. Karki, S.; Gohain, M.; Yadav, D.; Thakare, N.; Pawar, R.; Hazarika, S.; Ingole, P. Building rapid water transport channels within thin-film nanocomposite membranes based on 2D mesoporous nanosheets. *Desalination* **2023**, *547*, 116222. [CrossRef]
103. Li, X.; Zhao, C.; Yang, M.; Yang, B.; Hou, D.; Wang, T. Reduced graphene oxide-NH_2 modified low pressure nanofiltration composite hollow fiber membranes with improved water flux and antifouling capabilities. *Appl. Surf. Sci.* **2017**, *419*, 418–428. [CrossRef]
104. Zhang, W.; Shi, M.; Heng, Z.; Zhang, W.; Pan, B. Soft Particles Enable Fast and Selective Water Transport through Graphene Oxide Membranes. *Nano Lett.* **2020**, *20*, 7327–7332. [CrossRef] [PubMed]
105. Chen, L.; Shi, G.; Shen, J.; Peng, B.; Zhang, B.; Wang, Y.; Bian, F.; Wang, J.; Li, D.; Qian, Z.; et al. Ion sieving in graphene oxide membranes via cationic control of interlayer spacing. *Nature* **2017**, *550*, 380–383. [CrossRef] [PubMed]
106. Côté, A.; Benin, A.; Ockwig, N.; O'Keeffe, M.; Matzger, A.; Yaghi, O. Porous, crystalline, covalent organic frameworks. *Science* **2005**, *310*, 1166–1170. [CrossRef] [PubMed]
107. Zhang, C.; Wu, B.; Ma, M.; Wang, Z.; Xu, Z. Ultrathin metal/covalent–organic framework membranes towards ultimate separation. *Chem. Soc. Rev.* **2019**, *48*, 3811–3841. [CrossRef] [PubMed]
108. Wang, H.; Zeng, Z.; Xu, P.; Li, L.; Zeng, G.; Xiao, R.; Tang, Z.; Huang, D.; Tang, L.; Lai, C.; et al. Recent progress in covalent organic framework thin films, fabrications, applications and perspectives. *Chem. Soc. Rev.* **2019**, *48*, 488–516. [CrossRef] [PubMed]
109. Diercks, C.; Yaghi, O. The atom, the molecule, and the covalent organic framework. *Science* **2017**, *355*, aal1585. [CrossRef]
110. Wang, J.; Zhuang, S. Covalent organic frameworks (COFs) for environmental applications. *Coordin. Chem. Rev.* **2019**, *400*, 213046. [CrossRef]
111. Yuan, S.; Li, X.; Zhu, J.; Zhang, G.; Puyveldeb, P.; Bruggen, B. Covalent organic frameworks for membrane separation. *Chem. Soc. Rev.* **2019**, *48*, 2665–2681. [CrossRef]
112. Sui, X.; Yuan, Z.; Liu, C.; Wei, L.; Xu, M.; Liu, F.; Montoya, A.; Goh, K.; Chen, Y. Graphene oxide laminates intercalated with 2D covalent-organic frameworks as a robust nanofiltration membrane. *J. Mater. Chem. A* **2020**, *8*, 9713–9725. [CrossRef]
113. Zhang, Y.; Guo, J.; Han, G.; Bai, Y.; Ge, Q.; Ma, J.; Lau, C.; Shao, L. Molecularly soldered covalent organic frameworks for ultrafast precision sieving. *Sci. Adv.* **2021**, *7*, abe8706. [CrossRef] [PubMed]
114. Yuan, B.; Wang, M.; Wang, B.; Yang, F.; Quan, X.; Tang, C.; Dong, Y. Cross-linked Graphene Oxide Framework Membranes with Robust Nano-Channels for Enhanced Sieving Ability. *Environ. Sci. Technol.* **2020**, *54*, 15442–15453. [CrossRef] [PubMed]
115. Wu, M.; Yuan, J.; Wu, H.; Su, Y.; Yang, H.; You, X.; Zhang, R.; He, X.; Khan, N.; Kasher, R.; et al. Ultrathin nanofiltration membrane with polydopamine-covalent organic framework interlayer for enhanced permeability and structural stability. *J. Membr. Sci.* **2019**, *576*, 131–141. [CrossRef]
116. Zhu, J.; Qin, L.; Uliana, A.; Hou, J.; Wang, J.; Zhang, Y.; Li, X.; Yuan, S.; Li, J.; Tian, M.; et al. Elevated performance of thin film nanocomposite membranes enabled by modified hydrophilic MOFs for nanofiltration. *ACS Appl. Mater. Interfaces* **2017**, *9*, 1975–1986. [CrossRef]
117. Pang, J.; Kang, Z.; Wang, R.; Xu, B.; Nie, X.; Fan, L.; Zhang, F.; Du, X.; Feng, S.; Sun, D. Exploring the sandwich antibacterial membranes based on UiO-66/graphene oxide for forward osmosis performance. *Carbon* **2019**, *144*, 321–332. [CrossRef]
118. Zhang, W.; Yin, M.; Zhao, Q.; Jin, C.; Wang, N.; Ji, S.; Ritt, C.; Elimelech, M.; An, Q. Graphene oxide membranes with stable porous structure for ultrafast water transport. *Nat. Nanotechnol.* **2021**, *16*, 337–343. [CrossRef] [PubMed]
119. Chen, J.; Li, Z.; Wang, C.; Wu, H.; Liu, G. Synthesis and characterization of g-C_3N_4 nanosheet modified polyamide nanofiltration membranes with good permeation and antifouling properties. *RSC Adv.* **2016**, *6*, 112148–112157. [CrossRef]
120. Wang, Y.; Li, L.; Wei, Y.; Xue, J.; Chen, H.; Ding, L.; Caro, J.; Wang, H. Water transport with ultralow friction through partially exfoliated g-C_3N_4 nanosheet membranes with self-supporting spacers. *Angew. Chem. Int. Edit.* **2017**, *56*, 8974–8980. [CrossRef]

121. Wang, Y.; Liu, L.; Hong, J.; Cao, J.; Deng, C. A novel $Fe(OH)_3$/g-C_3N_4 composite membrane for high efficiency water purification. *J. Membr. Sci.* **2018**, *564*, 372–381. [CrossRef]
122. Ye, W.; Liu, H.; Lin, F.; Lin, J.; Zhao, S.; Yang, S.; Hou, J.; Zhou, S.; Bruggen, B. High-flux nanofiltration membranes tailored by bio-inspired co-deposition of hydrophilic g-C_3N_4 nanosheets for enhanced selectivity towards organics and salts. *Environ. Sci. Nano* **2019**, *6*, 2958–2967. [CrossRef]
123. Li, Z.; Xing, Y.; Fan, X.; Lin, L.; Meng, A.; Li, Q. rGO/protonated g-C_3N_4 hybrid membranes fabricated by photocatalytic reduction for the enhanced water desalination. *Desalination* **2018**, *443*, 130–136. [CrossRef]
124. Naguib, M.; Kurtoglu, M.; Presser, V.; Lu, J.; Niu, J.; Heon, M.; Hultman, L.; Gogotsi, Y.; Barsoum, M. Two-dimensional nanocrystals produced by exfoliation of Ti_3AlC_2. *Adv. Mater.* **2011**, *23*, 4248–4253. [CrossRef] [PubMed]
125. Liang, B.; He, X.; Hou, J.; Li, L.; Tang, Z. Membrane separation in organic liquid: Technologies, achievements, and opportunities. *Adv. Mater.* **2019**, *31*, 1806090. [CrossRef] [PubMed]
126. Ding, L.; Wei, Y.; Wang, Y.; Chen, H.; Caro, J.; Wang, H. A two-dimensional lamellar membrane: MXene nanosheet stacks. *Angew. Chem. Int. Edit.* **2017**, *56*, 1825–1829. [CrossRef] [PubMed]
127. Wu, X.; Hao, L.; Zhang, J.; Zhang, X.; Wang, J.; Liu, J. Polymer-$Ti_3C_2T_x$ composite membranes to overcome the trade-off in solvent resistant nanofiltration for alcohol-based system. *J. Membr. Sci.* **2016**, *515*, 175–188. [CrossRef]
128. Jiang, J.; Bai, S.; Zou, J.; Liu, S.; Hsu, J.; Li, N.; Zhu, G.; Zhuang, Z.; Kang, Q.; Zhang, Y. Improving stability of MXenes. *Nano Res.* **2022**, *15*, 6551–6567. [CrossRef]
129. Mishra, A.; Srivastava, P.; Carreras, A.; Tanaka, I.; Mizuseki, H.; Lee, K.; Singh, A. Atomistic origin of phase stability in oxygen-functionalized MXene: A comparative study. *J. Phys. Chem. C* **2017**, *121*, 18947–18953. [CrossRef]
130. Bi, R.; Zhang, Q.; Zhang, R.; Su, Y.; Jiang, Z. Thin film nanocomposite membranes incorporated with graphene quantum dots for high flux and antifouling property. *J. Membr. Sci.* **2018**, *553*, 17–24. [CrossRef]
131. Long, L.; Wu, C.; Yang, Z.; Tang, C. Carbon Nanotube Interlayer Enhances Water Permeance and Antifouling Performance of Nanofiltration Membranes: Mechanisms and Experimental Evidence. *Environ. Sci. Technol.* **2022**, *56*, 2656–2664. [CrossRef]
132. Safarpour, M.; Vatanpour, V.; Khataee, A.; Esmaeili, M. Development of a novel high flux and fouling-resistant thin film composite nanofiltration membrane by embedding reduced graphene oxide/TiO_2. *Sep. Purif. Technol.* **2015**, *154*, 96–107. [CrossRef]
133. Abdi, G.; Alizadeh, A.; Zinadini, S.; Moradi, G. Removal of dye and heavy metal ion using a novel synthetic polyethersulfone nanofiltration membrane modified by magnetic graphene oxide/metformin hybrid. *J. Membr. Sci.* **2018**, *552*, 326–335. [CrossRef]
134. Meng, N.; Zhao, W.; Shamsaei, E.; Wang, G.; Zeng, X.; Lin, X.; Xu, T.; Wang, H.; Zhang, X. A low-pressure GO nanofiltration membrane crosslinked via ethylenediamine. *J. Membr. Sci.* **2018**, *548*, 363–371. [CrossRef]
135. Gholami, F.; Ghanizadeh, G.; Zinatizadeh, A.; Zinadini, S.; Masoumbeigi, H. Arsenic and total dissolved solids removal using antibacterial/antifouling nanofiltration membranes modified by functionalized graphene oxide and copper ferrodioxide. *Water Environ. Res.* **2023**, *95*, e10902. [CrossRef] [PubMed]
136. Wang, Y.; Gao, B.; Yue, Q.; Wang, Z. Graphitic carbon nitride (g-C_3N_4)-based membranes for advanced separation. *J. Mater. Chem. A* **2020**, *8*, 19133–19155. [CrossRef]
137. Abdikheibari, S.; Lei, W.; Dumée, L.; Milne, N.; Baskaran, K. Thin film nanocomposite nanofiltration membranes from amine functionalized-boron nitride/polypiperazine amide with enhanced flux and fouling resistance. *J. Mater. Chem. A* **2018**, *6*, 12066–12081. [CrossRef]
138. Madhoush, M.R.; Sarrafzadeh, M.H.; Hosseinian, A. Molecular insight into water desalination mechanism through g-C_3N_4 nano-slit membranes: Effect of slit sizes, terminal groups, and number of layers. *J. Mol. Liq.* **2023**, *392*, 123532. [CrossRef]
139. Zou, X.Y.; Li, M.S.; Zhou, S.Y.; Chen, C.L.; Zhong, J.; Xue, A.L.; Zhang, Y.; Zhao, Y.J. Diffusion behaviors of ethanol and water through g-C3N4-based membranes: Insights from molecular dynamics simulation. *J. Membr. Sci.* **2019**, *585*, 81–89. [CrossRef]